

Observational estimates of the horizontal eddy diffusivity and mixing length in the low-level region of intense hurricanes

Jun A. Zhang^{1,2*} and Michael T. Montgomery^{2,3}

¹ *Rosenstiel School of Marine and Atmospheric Science, University of Miami, Miami, Florida*

² *NOAA/AOML/ Hurricane Research Division, Miami, Florida*

³ *Naval Postgraduate School, Department of Meteorology, Monterey, California*

November, 2011

Resubmitted to Journal of the Atmospheric Sciences

*Correspondence author: Dr. Jun Zhang, NOAA/AOML/Hurricane Research Division, 4301 Rickenbacker Causeway, Miami, FL 33149, E-mail jun.zhang@noaa.gov

Report Documentation Page

Form Approved
OMB No. 0704-0188

Public reporting burden for the collection of information is estimated to average 1 hour per response, including the time for reviewing instructions, searching existing data sources, gathering and maintaining the data needed, and completing and reviewing the collection of information. Send comments regarding this burden estimate or any other aspect of this collection of information, including suggestions for reducing this burden, to Washington Headquarters Services, Directorate for Information Operations and Reports, 1215 Jefferson Davis Highway, Suite 1204, Arlington VA 22202-4302. Respondents should be aware that notwithstanding any other provision of law, no person shall be subject to a penalty for failing to comply with a collection of information if it does not display a currently valid OMB control number.

1. REPORT DATE NOV 2011		2. REPORT TYPE		3. DATES COVERED 00-00-2011 to 00-00-2011	
4. TITLE AND SUBTITLE Observational estimates of the horizontal eddy diffusivity and mixing length in the low-level region of intense hurricanes				5a. CONTRACT NUMBER	
				5b. GRANT NUMBER	
				5c. PROGRAM ELEMENT NUMBER	
6. AUTHOR(S)				5d. PROJECT NUMBER	
				5e. TASK NUMBER	
				5f. WORK UNIT NUMBER	
7. PERFORMING ORGANIZATION NAME(S) AND ADDRESS(ES) Naval Postgraduate School, Department of Meteorology, Monterey, CA, 93943				8. PERFORMING ORGANIZATION REPORT NUMBER	
9. SPONSORING/MONITORING AGENCY NAME(S) AND ADDRESS(ES)				10. SPONSOR/MONITOR'S ACRONYM(S)	
				11. SPONSOR/MONITOR'S REPORT NUMBER(S)	
12. DISTRIBUTION/AVAILABILITY STATEMENT Approved for public release; distribution unlimited					
13. SUPPLEMENTARY NOTES					
14. ABSTRACT This study examines further the characteristics of turbulent flow in the low-level region of intense hurricanes using in-situ aircraft observations. The data analyzed here are the flight-level data collected by research aircraft that penetrated the eyewalls of Category 5 Hurricane Hugo (1989), Category 4 Hurricane Allen (1980) and Category 5 Hurricane David (1979) between 1 km and the sea surface. Estimates of horizontal eddy momentum flux, horizontal eddy diffusivity and horizontal mixing length are obtained. It is found that the horizontal momentum flux and horizontal diffusivity increase with increasing wind speed. The horizontal mixing length increases slightly with wind speed also, but the mixing length is not significantly dependent on the wind speed. The magnitude of the horizontal momentum flux is found to be comparable to that of the vertical momentum flux, indicating that horizontal mixing by turbulence becomes non-negligible in the hurricane boundary layer, especially in the eyewall region. Within the context of simple K-theory, the results suggest that the average horizontal eddy diffusivity and mixing length are approximately 1500 m² s⁻¹ and 750 m, respectively, at ~500 m in the eyewall region corresponding to the mean wind speed of approximately 52 m s⁻¹. It is recalled also that the mixing length is a virtual scale in numerical models, and is quantitatively smaller than the energy-containing scale of turbulent eddies. The distinction between these two scales is a useful reminder for the modeling community on the representation of small-scale turbulence in hurricanes.					
15. SUBJECT TERMS					
16. SECURITY CLASSIFICATION OF:			17. LIMITATION OF ABSTRACT	18. NUMBER OF PAGES	19a. NAME OF RESPONSIBLE PERSON
a. REPORT unclassified	b. ABSTRACT unclassified	c. THIS PAGE unclassified			

ABSTRACT

This study examines further the characteristics of turbulent flow in the low-level region of intense hurricanes using in-situ aircraft observations. The data analyzed here are the flight-level data collected by research aircraft that penetrated the eyewalls of Category 5 Hurricane Hugo (1989), Category 4 Hurricane Allen (1980) and Category 5 Hurricane David (1979) between 1 km and the sea surface. Estimates of horizontal eddy momentum flux, horizontal eddy diffusivity and horizontal mixing length are obtained. It is found that the horizontal momentum flux and horizontal diffusivity increase with increasing wind speed. The horizontal mixing length increases slightly with wind speed also, but the mixing length is not significantly dependent on the wind speed. The magnitude of the horizontal momentum flux is found to be comparable to that of the vertical momentum flux, indicating that horizontal mixing by turbulence becomes non-negligible in the hurricane boundary layer, especially in the eyewall region.

Within the context of simple K-theory, the results suggest that the average horizontal eddy diffusivity and mixing length are approximately $1500 \text{ m}^2 \text{ s}^{-1}$ and 750 m, respectively, at ~500 m in the eyewall region corresponding to the mean wind speed of approximately 52 m s^{-1} . It is recalled also that the mixing length is a virtual scale in numerical models, and is quantitatively smaller than the energy-containing scale of turbulent eddies. The distinction between these two scales is a useful reminder for the modeling community on the representation of small-scale turbulence in hurricanes.

Key words: Hurricane, typhoon, boundary layer, turbulent fluxes, spectra, horizontal eddy diffusivity, horizontal mixing length

1. Introduction

Turbulent transport processes in the boundary layer are believed to play an important role in the intensification and maintenance of a tropical cyclone (e.g., Emanuel 1995, Emanuel 1997, Wroe and Barnes 2003, Persing and Montgomery 2003, Smith et al. 2008, Davis et al. 2008, Bryan and Rotunno, 2009, Rotunno et al. 2009, Smith et al. 2009, Smith and Montgomery 2010, Montgomery and Smith 2011). The reason is in part because boundary layer turbulent fluxes modulate the uptake of enthalpy from the ocean and the loss of absolute angular momentum into the ocean. Because the horizontal grid spacing of current operational numerical models (> 3 km) for hurricane simulation and forecast is generally much larger than the scales of turbulent eddies (100 – 1000 m), the turbulent transport of energy and momentum have to be parameterized. In order to link turbulent quantities to mean variables it is standard to use the so called sub-grid scale parameterization schemes, such as the surface layer and planetary boundary layer (PBL) schemes in numerical models.

The parameterization of turbulent flux in the atmospheric boundary layer is often achieved through a simple eddy diffusivity closure model, also called “K-theory” (e.g., Eliassen 1971, Eliassen and Lystad 1977, Braun and Tao 2000, Kepert and Wang 2001, Holton 2004, Nolan et al. 2009 a, b, Foster 2009, Smith and Thomsen 2010). In low wind conditions, the horizontal momentum flux is usually assumed to be much smaller than the vertical momentum flux (e.g., Malkus and Riehl 1960). For this reason, vertical transport of turbulent momentum flux has received more attention in the boundary layer community than the horizontal transport. There have been extensive studies on the vertical transport of momentum and heat in low to moderate wind speed conditions (e.g., Hanna 1968, O’Brien 1970, Troen and Mahrt 1986, Hunt 1985, Hotslag and Moeng 1991, Lee 1996, Noh et al. 2003). Nonetheless, observational data are

scarce under major hurricane conditions, and the quantitative value and variation with wind speed of the vertical and horizontal eddy diffusivities remain poorly understood.

Using the data from the periods of eyewall penetrations in the intense Hurricanes Hugo (1989) and Allen (1980), Zhang et al. (2011a, ZM11 hereafter) obtained the first estimate of vertical momentum flux and the corresponding vertical eddy diffusivity in the inflow layer in intense hurricanes. These authors found that the vertical eddy diffusivity is on the order of $100 \text{ m}^2 \text{ s}^{-1}$ at $\sim 500 \text{ m}$ in the intense eyewall with flight-level mean wind speed up to 65 m s^{-1} . They found also that the vertical eddy diffusivity increases with increasing wind speed at a similar altitude.

It was not until relatively recently that horizontal momentum diffusion was suggested to be an important element in both the theory and numerical simulation of hurricane intensification and the maximum possible intensity (Emanuel 1989, 1997; Bryan and Rotunno 2009, BR09 hereafter; Bryan et al. 2010). In particular, using an axisymmetric numerical cloud model the latter authors demonstrated that the maximum intensity of their simulated hurricanes was very sensitive to the configuration of horizontal mixing length. It is of interest to note at this point that no previous study has given the value of horizontal mixing length based on observational data under hurricane conditions.

The purpose of this paper is to extend the ZM11 study by providing new estimates of the horizontal diffusivity and mixing length in the hurricane boundary layer for major hurricanes. Again, we use the data in Hurricanes Hugo (1989) and Allen (1980). In addition, we analyze another dataset which was collected in the low-level region of Category 5 Hurricane David (1979). In order to provide useful guidance to the modeling community charged with improving the forecast of hurricane intensity, we will quantify the mixing length of horizontal eddy

momentum flux. An outline of the remaining sections of this paper is as follows. In section 2, we give a brief description of data used and the analysis methodology. In section 3, we present the results of the data analysis. This is followed by Section 4, which discusses the main findings and the limitations of our results. Section 5 shortly summarizes the conclusion and future work.

2. Data and analysis method

As mentioned earlier, the data used in this study are mainly from three research flights, one into category 4 Hurricane Allen (1980), one into category 5 Hurricane David (1979), and the other in category 5 Hurricane Hugo (1989). We analyzed the flight-level data from the period of missions before and during the eyewall penetrations when NOAA research aircraft were flown at nearly constant radar altitudes below 1 km. Wind velocity data were corrected for aircraft motion, measured with an Inertial Navigation System (INS) and Global Positioning System (GPS). Note that more advanced turbulence sensors were installed in N43RF, including the Rosemount turbulence gust probes in 1990s and Best aircraft turbulence (BAT) probe in 2000s (Drennan et al. 2007, French et al. 2007). Table 1 summarizes the measurements and calculations for the time intervals of the flights into Hurricanes Allen, David and Hugo. Overall, the time-averaged mean wind speeds obtained at flight level vary from 7 to 65 m s⁻¹.

The data from the flight into Hurricane Hugo on August 15, 1989 and from the flight into Hurricane Allen on August 6, 1980 have been described in detail by ZM11. Below we describe the data from the flight in Hurricane David (1979). Hurricane David (1979) formed from a tropical wave on August 22 and developed into a tropical depression on August 25 in the central Atlantic. David strengthened from a tropical storm on August 26, becoming a hurricane on August 27. As it moved west-northwestward, David rapidly intensified to a major hurricane on

August 27-28. After slightly weakening on August 29, David continued moving west-northwest, and became a Category 5 hurricane in the northeast Caribbean Sea. The peak intensity of Hurricane David reached maximum sustained winds of 78 m s^{-1} and minimum central pressure of 924 mb (hPa) on August 30. Hurricane David continued as a Category 5 hurricane on August 31.

On August 30 1979, NOAA research aircraft N43RF penetrated the eyewall of the Cat 5 Hurricane David (1979). Figure 1 summarizes the period of the flight during the low-level eyewall penetration mission. The aircraft altitude is nearly constant at 450 m, which is similar to the Hugo flight. Four eyewall penetrations were conducted, with peak flight-level wind speeds reaching 80 ms^{-1} . The gray lines in Fig. 1 at the bottom of each panel represent the time intervals selected to determine the scales of turbulent eddies and turbulence parameters. There is a total of thirteen time intervals (or 'flux runs') selected for analysis, four of which are in the eyewall region. Note that all of the time intervals are chosen according to the spectral analysis and quasi-stationary criterion as discussed and justified in detail by ZM11.

Similar to the two flights each in Hurricane Allen and Hugo, the flight into Hurricane David was mainly within the strong frictional inflow layer as discussed by ZM11. Upon analyzing hundreds of the dropsonde measurements in hurricanes, Zhang et al. (2011b) found recently that this layer of strong inflow adequately represents the top of the hurricane boundary layer, consistent with numerical and theoretical studies by Smith et al. (2009), Smith and Montgomery (2010) and Kepert (2011). On the basis of these recent works, the flights into Hurricanes Allen, David and Hugo are believed to be within the hurricane boundary layer as defined by the layer of strong inflow.

In general, the turbulent eddy momentum flux is a second order tensor. Since ZM11 have examined already the vertical eddy momentum flux components, we confine our attention here to

the horizontal components of the eddy stress tensor. For the purpose of estimating horizontal mixing length, the horizontal momentum flux at flight level is evaluated for each time interval as follows:

$$F_h = -\rho \overline{(u'v')}, \quad (1)$$

where prime indicates a turbulent fluctuation, v and u represent latitudinal and longitudinal component velocities, ρ the air density, and the overbar represents a time-average operator.

Turbulent fluctuations are determined by detrending the time series of the three wind components using a least-square fitting method. A high-pass filter with a cutoff at 0.01 Hz was applied before the detrending. When we calculate ρ , we use the temperature measured by the Rosemont temperature sensor. It has been reported by Eastin et al. (2002a, b) that there is usually a wetting error in the temperature data during eyewall penetrations. The wetting error was corrected following the Eastin et al. method. The influence of the wetting error on the density calculation was found to be very small ($\sim 1\%$), nearly negligible.

The horizontal momentum flux is typically parameterized using the eddy diffusivity (K_h) in the form of

$$F_h = \rho K_h S_h, \quad (2)$$

where S_h is the strain rate of the mean flow (e.g., Stevens et al. 1999), which is defined as

$$S_h = \left(\frac{\partial v}{\partial x} + \frac{\partial u}{\partial y} \right), \quad (3)$$

where x and y are the distances to the storm center in longitudinal and latitudinal directions, respectively.

The horizontal eddy diffusivity can be calculated from (2) in the form of

$$K_h = |F_h| / (\rho |S_h|). \quad (4)$$

The horizontal mixing length is then determined from the horizontal eddy diffusivity and the deformation, in the form of

$$L_h = (K_h D_h^{-1})^{1/2}. \quad (5)$$

Here, D_h is the horizontal deformation and is defined as

$$D_h^2 = \left(\frac{\partial v}{\partial x} + \frac{\partial u}{\partial y}\right)^2 + \left(\frac{\partial u}{\partial x} - \frac{\partial v}{\partial y}\right)^2. \quad (6)$$

The first term in rhs of Eq. (6) represents deformation due to shearing, while the second term represents deformation due to stretching.

We note that in the above equations (1-6), the horizontal eddy momentum flux and strain rate can take on either positive or negative values around the storm, while the horizontal eddy diffusivity and mixing length must be positive for physical consistency. This sign convention for eddy diffusivity and mixing length is based on the K-theory. Since the purpose of this paper is to estimate the horizontal eddy diffusivity and mixing length, we have used the magnitudes of the momentum flux and strain rate when calculating the eddy diffusivity (see Eq. 4). On the other hand, the signs of momentum flux and strain rate are reported (see Table 1) and discussed in the context of the applicability of K-theory in Sections 3 and 4.

The uncertainty involved in the estimation of horizontal eddy momentum flux is from two parts: 1) the temporal resolution of the data used in the calculation is 1 Hz, which generally will not capture the entire spectrum of the turbulent kinetic energy; 2) the legs determined for the flux calculation are relatively short (e.g., ~ 20 km) due to the quality control requirement for statistical stationarity. ZM11 discussed in detail how the 1 Hz data may under-sample the turbulent energy and fluxes.

In this work, we take the same approach as used by ZM11 to correct the 1 Hz data in Hurricanes Allen, David and Hugo using the 40 Hz data from Hurricane Frances (2004) at a

similar altitude. The data in Hurricane Frances were collected during the Coupled Boundary Layer Air-sea Transfer (CBLAST) Hurricane experiment (Black et al. 2007, Zhang et al. 2008). We found that the 1 Hz Frances data captures approximately 80% of the total horizontal eddy momentum flux (Fig.3). Therefore, in the analysis of the Allen, David and Hugo data, this empirical correction is applied also. In the correction, we have assumed that the turbulence characteristics at the vertical levels and locations in Frances, Hugo and Allen behave similarly. We recognize that there is an uncertainty in the correction, especially in the eyewall region where the 40 Hz data is unavailable, but this approach provides our best estimates. The short time interval used in the calculations can yield uncertainty of variance and covariance fluxes according to Mann and Lenschow (1994) and Mahrt (1998). A detailed error analysis is given in section 3 where the main results are presented.

In the calculation of the strain rate and deformation using Eqs (3) and (6), errors are introduced from the required cross-track derivatives since the data used here are from single flight legs. Since the aircraft horizontal track is never along the east or west direction, it is believed that errors due to the cross-track derivative are not overly significant, if homogeneity is assumed within the area that covers the flux run. Nonetheless, to improve the accuracy of our analysis we make the reasonable approximation of an axisymmetric mean vortex flow in order to evaluate the mean strain rate. We thus rewrite Eqs. (3) and (5) in the cylindrical coordinates, as follows:

$$S_h = \left(\frac{\partial v_t}{\partial r} - \frac{v_t}{r}\right) \cos 2\lambda + \left(\frac{\partial v_r}{\partial r} - \frac{v_r}{r}\right) \sin 2\lambda, \quad (7)$$

$$D_h^2 = 2\left(\frac{\partial v_r}{\partial r}\right)^2 + 2\left(\frac{v_r}{r}\right)^2 + \left(\frac{\partial v_t}{\partial r} - \frac{v_t}{r}\right)^2, \quad (8)$$

where v_r and v_t are the radial and tangential components of the velocity (assumed to depend on radius only), r is the radius to the storm center, and λ is the azimuth angle with $\lambda=0$ defined to be due east. As all the flux runs selected in the analyses are nearly along the radial direction of the storm, the foregoing estimation of the mean strain rate and deformation avoids the problem of needing cross-track derivatives and for this reason is considered a more robust and defensible estimate of the mean strain rate and deformation than Eqs. (3) and (5). In the upcoming analyses we will henceforth use the cylindrical coordinate forms, Eqs. (7) and (8).

3. Results

The calculations of horizontal eddy momentum flux, eddy diffusivity and mixing length are summarized in Tables 1 for the Allen, David and Hugo data. The calculations of the turbulence parameters outside the eyewalls of these storms show good agreement with those using the 40 Hz Frances data. This agreement suggests that the method employed for correcting the 1 Hz data is sound. The mean horizontal momentum flux for the eyewall penetration legs¹ is approximately $1.5 \text{ m}^2 \text{ s}^{-2}$ with a flight-level mean wind speed of 52 m s^{-1} . Broadly speaking, the horizontal momentum fluxes in the eyewall legs are generally 5 times those found in the outer core runs.

Figure 4 shows the horizontal momentum flux as a function of the flight-level mean wind speed using the data from Hurricanes Allen, David and Hugo. Also shown are the values of horizontal momentum fluxes determined from the 40 Hz data obtained in Hurricane Frances. It is evident that the horizontal momentum flux increases with the increasing flight-level wind speed.

¹ Here the eyewall region is defined as the area within 30 km of the radius of maximum wind.

This wind-speed dependence of horizontal momentum flux is qualitatively similar to the wind-speed dependence of vertical momentum flux reported by ZM11.

It appears that the magnitude of horizontal momentum flux becomes roughly comparable to the vertical momentum flux close to and inside the eyewall region (Fig. 5). In the corner-flow region of the vortex where the mean inflow is decelerating and turning upwards and the radial and height scales become comparable, this suggests that the horizontal mixing may become non-negligible compared to the vertical mixing processes in the underlying boundary layer dynamics of the vortex. The implication is that the divergence of the horizontal eddy momentum flux should not be neglected in theory or hurricane models. An estimate of the horizontal eddy diffusivity will follow after error sources are considered.

As mentioned in Section 2, there are sources of error that are involved in the flux estimation. Typically, two types of errors arise in the flux calculation using the eddy-correlation method: the systematic error (erS), which is linked to the loss due to high-pass filtering; and random error (erR), which is due to the fact that a flux run is a finite sample of a random process. We calculate the systematic error for the flux estimation following Lenschow et al. (1994) in the form of:

$$\text{erS} = (F - F_f) / F, \quad (7)$$

where F_f is the flux after application of the high pass filter in the frequency domain. The systematic error is found to be 31%, which is typical for aircraft observations especially at these altitudes (e.g. Bernard-Trottolo et al. 2003). We calculate the random error following Vickers and Mahrt (1997) in the form of:

$$\text{erR} = \sigma_F / \bar{F} / \sqrt{N}, \quad (8)$$

where N is the number of observations. The random error is found to be 25%, which is in agreement with values found in the previous aircraft observations (e.g., Mann and Leschow 1994, Bernard-Trottolo et al. 2003). Because all of the flux runs were checked thoroughly using the ‘ogive’ criterion and spectral analysis method as mentioned in Section 3 (and detailed in ZM11), all of the low-frequency scales of turbulent eddies are believed to be captured. We have corrected also the missing high frequency part of the energy based on the Frances data. Overall, it is thought that the uncertainty of the estimated horizontal momentum flux is around 30%.

Figure 6 shows the horizontal eddy diffusivity derived from Equation (4) as a function of the mean flight-level wind speed, using the Allen, David and Hugo data, as well as the 40 Hz Frances data. Again, we find that the Allen, David and Hugo data in the outer core region are consistent with the Frances data, providing an independent check of the validity of the bias correction. In the eyewall region, the average horizontal eddy diffusivity is approximately $1500 \text{ m}^2 \text{ s}^{-1}$, which is slightly more than an order of magnitude greater than the vertical eddy diffusivity as given by ZM11. Considering all the data investigated in this work, it is evident that the horizontal eddy diffusivity in the eyewall region is nearly twice as large as that found in the outer core region. Overall, it is found that the eddy diffusivity tends to increase with increasing mean flight-level wind speed.

Adopting a K theory closure formulation, the horizontal mixing length is computed from the horizontal eddy diffusivity and the deformation following Eq. (5). Figure 7 shows the horizontal mixing length as a function of mean flight-level wind speed for all of the flux runs. The average horizontal mixing length of the eyewall legs is approximately 750 m, corresponding to a mean wind speed of 52 ms^{-1} . The mixing length of the outer-core legs is approximately 630

m. It appears, then, that the horizontal mixing length has little dependence on the mean flight-level wind speed, with only a slight increasing trend with wind speed.

In the calculation of the horizontal eddy diffusivity, the determination of the mean strain rate term (S_h) is required. In the calculation of the horizontal mixing length, the calculation of the mean deformation (D_h) is required. Here, we calculate S_h and D_h using the flight-level wind data that is smoothed by a 100s running mean filter. This method is the same as used by Marks et al. (2008) for the determination of the mean vortex of Hurricane Hugo (1989). In the calculation of S_h and D_h for each flux run, we take the average value from all the observations in each leg. The uncertainty in the calculation of S_h and D_h comes mainly from the distance from the storm center. We have used the algorithm given by Willoughby and Chelmon (1980) to determine the storm center using the flight-level wind data. As discussed in the foregoing section, we have also corrected the cross-track error by rewriting S_h and D_h in the cylindrical coordinate system and assuming an axisymmetric mean vortex flow to evaluate the respective derivatives. The uncertainties in the estimates of S_h and D_h are thought to be within 20%. Overall, the uncertainties of the horizontal eddy diffusivity and mixing length are thought to be 50%. It is worthwhile to note that calculations of S_h and D_h using the two methods discussed in Section 2 are in general agreement (not shown). However, calculating S_h and D_h in the Cartesian coordinate system (Eqs. (3) and (5)) introduces much larger scatter than in the Cylindrical coordinate system (Eqs. (7) and (8)), with some unreasonably large values of K_h and L_h .

4. Discussion

In this study, we have extended the analyses of ZM11 examining the turbulence characteristics in the boundary layer of Hurricanes Allen (1980) and Hugo (1989). To

supplement the data base, we added an analysis of a similar dataset collected during the low-level eyewall penetrations of category 5 Hurricane David (1979). Estimates of the horizontal eddy momentum flux, horizontal eddy diffusivity, and horizontal mixing length were presented for the legs before and during the eyewall penetrations. The horizontal eddy momentum flux for the eyewall legs were found to be much larger than those estimated for the legs outside the eyewall at the same level. It was found also that the horizontal momentum flux increases with wind speed, qualitatively similar to the wind-speed dependence of the vertical momentum flux as presented by ZM11.

In the eyewall region, where the corresponding wind speed is equal to or greater than 52 ms^{-1} , the mean horizontal eddy diffusivity is found to be on the order of $1500 \text{ m}^2 \text{ s}^{-1}$, which is approximately 15 times that of the vertical eddy diffusivity reported in ZM11. The horizontal eddy diffusivity is found to increase somewhat with wind speed. The horizontal mixing length is approximately 750 m on average in the eyewall with a slightly smaller value ($\sim 630 \text{ m}$) in the outer core. There is a weak increase of the horizontal mixing length with wind speed. From both theoretical and practical perspectives, the observational evidence suggests that a constant horizontal mixing length may be adequate in simple theoretical models and in numerical hurricane models. The horizontal mixing length is approximately seven times the vertical mixing length.

Because the radial and vertical scales become comparable in the corner flow region of a major hurricane eyewall, our results suggest that the flux divergence of the horizontal eddy momentum flux will become non-negligible in the boundary layer dynamics for this region of the storm. Although these conclusions are consistent with the statements of BR09, it must be noted that our estimated horizontal mixing length is smaller than the value of 1500 m suggested by

BR09 using an axisymmetric numerical model. This discrepancy can be partly explained by the limitation of a 2D axisymmetric model. As stated by BR09 (see their page 1776), “axisymmetric numerical models cannot resolve any three-dimensional motions.” The unresolved three-dimensional turbulence, including Kolmogorov and mesoscale turbulence associated with rotating deep convection, eyewall mesovortices and vortex Rossby waves (Rotunno and Emanuel 1987, Nguyen *et al.* 2008, Schubert *et al.* 1999, Montgomery *et al.* 2002, BR09) may be one reason for the above discrepancy. Cognizant of the limitations of the 2D (axisymmetric) model, Bryan, Rotunno and their colleagues (Bryan *et al.* 2010) suggested a somewhat smaller horizontal mixing length (~ 1000 m) to be the optimal length scale in order for that in their 3D simulations to match observed hurricane intensities. Their recommended mixing length from the 3D simulations is closer to our observational estimate compared to their 2D simulations.

We note that the data used in our analyses are based on flight level data at ~ 500 m altitude, which is close to the height of maximum wind speed. The height of the maximum tangential wind speed is generally slightly higher (Zhang *et al.* 2011b). A rough estimate of the azimuthal tangential wind speed using all the eyewall legs considered here is on the order of 52 m s^{-1} , which is smaller than the one ($\sim 70 \text{ m s}^{-1}$) used by BR09 and Bryan *et al.* (2010) as the baseline of their numerical simulation for recommending the horizontal mixing length. Given the tendency for the horizontal mixing length to increase slightly with wind speed, a 1000 m horizontal mixing length would appear to be a reasonable estimate at higher wind speeds. Undoubtedly, more observations at higher wind speeds and at different altitudes in intense eyewalls are required for a more complete understanding and representation of the turbulent mixing problem in hurricanes.

In our analysis of the observational turbulence data, we have recalled the fact that the mixing length is a virtual length scale and is generally different from the scale of turbulent eddies

containing most of the turbulent kinetic energy and momentum fluxes. In numerical models, for example, the mixing length concept is used to link the turbulent fluxes to more easily measured and resolved variables, such as wind shear and/or deformation rate (e.g., Pielke and Mahrer, 1975). In the real world, such length scales should be determined when both flux and mean profile data are available. On the other hand, the scales of dominant eddies can be determined using a spectral analysis (e.g. Zhang et al. 2009, Zhang 2010, ZM11).

As an example, Fig. 8a shows the cospectra of the horizontal momentum flux for one of the flux runs that penetrated the eyewall of category 5 Hurricane David. The corresponding cumulative sum or ogives of the cospectrum of horizontal momentum flux is shown in Figs. 8b. The dominant peaks in the cospectral plots are generally associated with turbulent eddies that contain most of the momentum flux. As in ZM11, the scale of the dominant eddies can be estimated from the reciprocal of the pertinent wavenumber. From Fig. 8, the peak of the uv cospectrum occurs at a wavenumber of approximately $0.95 \times 10^{-3} \text{ m}^{-1}$ and this wavenumber corresponds to a length scale of approximately 1100 m. Similar results are found for the other eyewall flux runs, and also for the outer-core runs. Overall, we find that the mean length scale of the dominant eddies transporting the horizontal momentum flux is approximately 1130 m on average, which is nearly 1.6 times the average value of the horizontal mixing length. Although the energy containing scale is almost within the error bar of the horizontal mixing length, statistical analysis (t-test) shows that the difference between the mean mixing length and energy/flux containing scale is significantly different. The distinction between these two scales is a useful reminder for the modeling community on the representation of small-scale turbulence in hurricanes.

We note also that the results presented here are framed within the context of simple K-theory and assume that such an approach is valid in hurricane conditions. Many numerical models of hurricanes (including the models employed by Bryan and Rotunno (2009, 2010) and Nguyen et al. (2008)) adopt a K-theory formulation for the turbulence closure problem. When correlating the momentum flux and the strain rate, we found that nearly 70% of the data have the same signs, confirming the assumed down-gradient character between the horizontal eddy momentum flux and the mean strain rate in K-theory (see Table 1). Although the work presented here broadly supports the hypothesis that simple K-theory is valid in intense hurricanes, further analyses are required to evaluate the applicability of K-theory at different altitudes. Of course, if a higher order turbulence parameterization scheme is used in a hurricane model, then still higher-order statistical moments of the turbulence are required. The latter alternative goes far beyond the scope of the current study. Finally, it should be remembered that a hurricane boundary layer near the eyewall region is far from a homogeneous regime. However, the horizontal homogeneity condition is necessary within the surface layer similarity theory and boundary layer K-theory concept.

5. Conclusions

In summary, our study is the first attempt to estimate the horizontal diffusivity and mixing length in the very high wind regime of a hurricane vortex using observational data. We believe that the results presented herein should offer useful guidance in both theoretical studies and numerical weather prediction efforts aimed at improving the understanding and forecast of hurricane intensity. The Allen, David and Hugo flight-level datasets analyzed in this study are believed to be the few available in-situ observations that were taken near or below 500 m during

the eyewall penetration of a Category 4 and 5 storms. It is unlikely that we may see such data in the near future because of safety constraints for manned aircraft to be flown at such low altitudes again in the boundary layer.

Our future work aims to increase the sampling size of the analysis of turbulent flow in the eyewall region by searching the 30-year HRD's aircraft database for more low-level flights than those used in this study. To more completely quantify turbulence characteristics in the intense eyewall and their impact on our understanding and prediction of hurricane intensification and maximum intensity, a focused field program is recommended also, possibly with unmanned platforms employing advanced turbulent sensors on board or using advanced remote sensing techniques.

Acknowledgements

The first author JZ was supported through the NOAA HFIP program. MTM acknowledges support from NOAA's Hurricane Research Division, the U.S. Office of Naval Research Grant No. N0001411WX20095 and the National Science Foundation AGS-0715426. Author JZ appreciates helpful discussions and encouragement from Frank Marks and Robert Rogers. He is grateful also to George Bryan and Richard Rotunno for helpful discussions and comments on this work during his visit to NCAR. We thank Neal Dorst for providing the storm track data for Hurricane Allen (1980). We also acknowledge Mark Donelan for helpful suggestions. We would like to give special acknowledgement to all the scientists and crew members who have been involved the Hurricane Research Division field program to help collect the data used in this study. Without their efforts, this work would have been impossible. Finally, we wish to acknowledge Roger Smith, and two anonymous reviewers for their substantive and highly perceptive comments that led to improvements of the paper.

References

- Bernard-Trottolo, S., B. Campistron, A. Druilhet, F. Lohou, and F. Said, 2003: TRAC98: Detection of coherent structures in a convective boundary layer using airborne measurements. *Bound.-Layer Meteorol.*, **111**, 181-224.
- Black, P. G., E. D'Asaro, W. M. Drennan, J. R. French, P. P. Niiler, T. B. Sanford, E. J. Terrill, E. J. Walsh and J. A. Zhang, 2007: Air-sea exchange in hurricanes: Synthesis of observations from the Coupled Boundary Layer Air-Sea Transfer experiment. *Bull. Amer. Meteorol. Soc.*, **88**, 357-374.
- Braun, S. A., and W.-K. Tao, 2000: Sensitivity of high-resolution simulations of Hurricane Bob (1991) to planetary boundary layer parameterizations. *Mon. Wea. Rev.*, **128**, 3941–3961.
- Bryan, G. H., and R. Rotunno, 2009: The maximum intensity of tropical cyclones in axisymmetry numerical model simulations. *Mon. Wea. Rev.*, **137**, 1770-1789.
- Bryan, G. H., R. Rotunno, and Y. Chen, 2010: The effects of turbulence on hurricane intensity. Preprints, *29th Conference on Hurricanes and Tropical Meteorology*, Amer. Meteor. Soc., Tucson, AZ, 8C.7.
- Davis, C., and Coauthors, 2008: Prediction of landfalling hurricanes with the Advanced Hurricane WRF model. *Mon. Wea. Rev.*, **136**, 1990-2005.
- Drennan, W. M., J. A. Zhang, J. R. French, C. McCormick, P. G. Black, 2007: Turbulent fluxes in the hurricane boundary layer, II. Latent heat fluxes. *J. Atmos. Sci.*, **64**, 1103-1115.
- Eastin, M. D., P. G. Black, and W. M. Gray, 2002: Flight-level thermodynamic instrument wetting errors in hurricanes. Part I: observations. *Mon. Wea. Rev.*, **130**, 825-841.
- Eastin, M. D., P. G. Black, and W. M. Gray, 2002: Flight-level thermodynamic instrument wetting errors in hurricanes. Part II: implications. *Mon. Wea. Rev.*, **130**, 842-851.

- Eliassen, A., 1971: On the Ekman layer in a circular vortex. *J. Met. Soc. Japan*, **49**, 784-789.
- Eliassen, A. and M. Lystad, 1977: The Ekman layer of a circular vortex. A numerical and theoretical study. *Geophysica Norvegica*, **7**, 1-16.
- Emanuel, K.A., 1989: The finite-amplitude nature of tropical cyclogenesis. *J. Atmos. Sci.*, **46**, 3431-3456.
- Emanuel, K. A., 1995: Sensitivity of tropical cyclones to surface exchange coefficients and a revised steady-state model incorporating eye dynamics. *J. Atmos. Sci.*, **52**, 3969-3976.
- Emanuel, K.A., 1997: Some aspects of hurricane inner-core dynamics and energetics. *J. Atmos. Sci.*, **54**, 1014-1026.
- French, J. R., W. M. Drennan, J. A. Zhang and P.G. Black, 2007: Turbulent fluxes in the hurricane boundary layer. Part I: Momentum flux. *J. Atmos. Sci.*, **63**, 1089-1102.
- Frisch, U., 1996: *Turbulence: The Legacy of A. N. Kolmogorov*. Cambridge University Press, 296 pp.
- Foster, R. C., 2009: Boundary-layer similarity under an axisymmetric, gradient wind vortex. *Boundary-Layer Meteor.*, **131**, 321-344.
- Hanna, S. R., 1968: A method of estimating vertical eddy transport in the planetary boundary layer using characteristics of the vertical velocity spectrum. *J. Atmos. Sci.*, **25**, 1026-1033.
- Holt, T., and S. Raman, 1988: A review and comparative evaluation of multilevel boundary layer parameterization for First-Order and turbulent kinetic energy closure schemes. *Rev. Geophys.*, **26**, 761-780.
- Holtstlag, A. A. M., and C. Moeng, 1991: Eddy diffusivity and countergradient transport in the convective atmospheric boundary layer. *J. Atmos. Sci.*, **48**, 1690-1698.

- Holtslag, A. A. M., E. van Meijgaard, and W. C. de Rooij, 1995: A comparison of boundary layer diffusion schemes in unstable conditions over land. *Boundary-Layer Meteorol.*, **76**, 69-95.
- Hong, S. Y. and H. L. Pan, 1996: Nonlocal boundary layer vertical diffusion in a medium-range forecast model. *Mon. Wea. Rev.*, **124**, 2322-2339.
- Hunt, J. C. R., 1985: Diffusion in the stably stratified atmospheric boundary layer. *J. Climate App. Meteor.*, **24**, 1187-1195.
- Kepert, J., and Y. Wang, 2001: The dynamics of boundary layer jets within the tropical cyclone core. Part II: Nonlinear Enhancement. *J. Atmos. Sci.*, **58**, 2485-2501.
- Lee, X., 1996: Turbulence spectra and eddy diffusivity over forests. *J. Appl. Meteo.*, **35**, 1307–1318.
- Mahrt, L., 1998: Flux sampling errors from aircraft and towers. *J. Atmos. Oceanic Technol.*, **15**, 416–429.
- Malkus, J. S., and H. Riehl, 1960: On the dynamics and energy transformations in steady-state hurricanes. *Tellus*, **12**, 1–20.
- Mann, J., and D. H. Lenschow, 1994: Errors in airborne flux measurements. *J. Geophys. Res.*, **99**, 14, 519–14, 526.
- Marks, F. D., P. G. Black, M. T. Montgomery, and R. W. Burpee, 2008: Structure of the eye and eyewall of Hurricane Hugo (1989). *Mon. Wea. Rev.*, **136**, 1237-1259.
- Montgomery, T. M., and R. K. Smith, 2011: Paradigms for tropical-cyclone intensification, *Q. J. R. Meteorol. Soc.*, Submitted.
- Montgomery, M. T., V. A. Vladimirov, and P. V. Denissenko, 2002: An experimental study on hurricane mesovortices. *J. Fluid Mech.*, 471, 1-32.

- Montgomery, M. T., M. M. Bell, S. Aberson, and M. Black, 2006: Hurricane Isabel (2003): New insights into the physics of intense storms. Part I. Mean vortex structure and maximum intensity estimate. *Bull. Amer. Meteorol. Soc.*, **87**, 1335-1347.
- Nguyen, V. S., R. K. Smith, and M. T. Montgomery, 2008: Tropical-cyclone intensification and predictability in three dimensions, *Q. J. R. Meteorol. Soc.*, **134**, (632), 563-582.
- Noh, Y., W. G. Cheon, S. Y. Hong, and S. Raasch, 2003: Improvement of the K-profile model for the planetary boundary layer based on large eddy simulation data. *Bound.-Layer Meteor.*, **107**, 421-427.
- Nolan D. S., J. A. Zhang, and D. P. Stern, 2009: Evaluation of planetary boundary layer parameterizations in tropical cyclones by comparison of in-situ data and high-resolution simulations of Hurricane Isabel (2003). Part I: Initialization, maximum winds, and outer core boundary layer structure. *Mon. Wea. Rev.*, **137**, 3651-3674.
- Nolan D. S., J. A. Zhang, and D. P. Stern, 2009: Evaluation of planetary boundary layer parameterizations in tropical cyclones by comparison of in-situ data and high-resolution simulations of Hurricane Isabel (2003). Part II: Inner core boundary layer and eyewall structure. *Mon. Wea. Rev.*, **137**, 3675-3698.
- O'Brien, 1970: A note on the vertical structure of the eddy exchange coefficient in the planetary boundary layer. *J. Atmos. Sci.*, **27**, 1213-1215.
- Persing J. and M. T. Montgomery, 2003: Hurricane superintensity. *J. Atmos. Sci.*, **60**, 2349-2371.
- Rotunno, R., and K.A. Emanuel, 1987: An air-sea interaction theory for tropical cyclones, Part II: Evolutionary study using axisymmetric nonhydrostatic numerical model. *J. Atmos. Sci.*, **44**, 542-561.
- Rotunno, R., Y. Chen, W. Wang, C. Davis, J. Dudhia and G. J. Holland, 2009: Large-eddy simulation of an idealized tropical cyclone. *Bull. Amer. Meteorol. Soc.*, **90**, 1783-1788.

- Schubert, W. H., M. T. Montgomery, R. K. Taft, T. A. Guinn, S. R. Fulton, J. P. Kossin, and J. P. Edwards, 1999: Polygonal eyewalls, asymmetric eye contraction, and potential vorticity mixing in hurricanes. *J. Atmos. Sci.*, **56**, 1197-1223.
- Smith, R. K., M. T. Montgomery, and S. V. Nguyen, 2009: Tropical cyclone spin-up revisited. *Quart. J. Roy Met. Soc.*, **135**, 1321–1335.
- Smith, R. K., and M. T. Montgomery, 2010: Hurricane boundary-layer theory. *Quart. J. Roy Met. Soc.*, **136**, 1665 – 1670.
- Smith, R. K., M. T. Montgomery, and S. Vogl, 2008: A critique of Emanuel’s hurricane model and potential intensity theory. *Quart. J. Roy. Meteorol. Soc.*, **134**, 551-561.
- Smith, R. K., and G. L. Thomsen, 2010: Dependence of tropical-cyclone intensification on the boundary layer representation in a numerical model. *Quart. J. Roy Met. Soc.*, in press.
- Stevens, B., C. Moeng, and P. P. Sullivan, 1999: Large-Eddy simulations of radiatively driven convection: sensitivities to the representation of small scales. *J. Atmos. Sci.*, **56**, 3963-3984.
- Troen, I., and L. Mahrt, 1986: A simple model of the atmospheric boundary layer: Sensitivity to surface evaporation. *Bound.-Layer Meteor.*, **37**, 129-148.
- Uhlhorn, E. W., P. G. Black, J. L. Franklin, M. Goodberlet, J. Carswell, and A. S. Goldstein, 2007: Hurricane surface wind measurements from an operational stepped frequency microwave radiometer, *Mon. Wea. Rev.*, **9**, 3070-3085.
- Vickers, D., and L. Mahrt, 1997: Quality control and flux sampling problems for tower and aircraft data. *J. Atm. Ocean. Technol.* **14**, 512–526.
- Willoughby, H. E., and M. Chelmow, 1982: Objective determination of hurricane tracks from aircraft observations. *Mon. Wea. Rev.*, **110**, 1198-1305.

- Wroe, D. R., and G. M. Barnes 2003: Inflow layer energetic of Hurricane Bonnie (1998) near landfall. *Mon. Wea.Rev.*, **131**, 1600-1612.
- Zhang, J. A., 2010: Spectra characteristics of turbulence in the hurricane boundary layer. *Quart. J. Roy. Meteor. Soc.*, DOI:10.1002/qj.610.
- Zhang, J. A., P. G. Black, J. R. French, and W. M. Drennan, 2008: First direct measurements of enthalpy flux in the hurricane boundary layer: The CBLAST results. *Geophysical Research Letters*, 35(11):L14813, doi:10.1029/2008GL034374.
- Zhang, J. A., W. M. Drennan, P. G. Black, and J. R. French, 2009: Turbulence structure of the hurricane boundary layer between the outer rain bands. *Journal of Atmospheric Science*, **66**, 2455-2467.
- Zhang, J.A., F.D. Marks, Jr., M.T. Montgomery, and S. Lorsolo, 2011a: An estimation of turbulent characteristics in the low-level region of intense Hurricanes Allen (1980) and Hugo (1989). *Mon. Wea. Rev.*, 139, 1447-1462.
- Zhang, J. A., R. F. Rogers, D. S. Nolan, and F. D. Marks, 2011b: On the characteristic height scales of the hurricane boundary layer. *Monthly Weather Review*, in press.

Figure captions:

Figure 1: Aircraft altitude (a) and flight-level wind speed (b) during Hurricane David on 6 August 1980, 8-12 UTC. The gray lines denote the flux runs investigated herein.

Figure 2: Aircraft tracks for the research flights into Hurricanes Allen (a), David (b), Hugo (c), and Frances (d).

Figure 3: Comparison of the 40 Hz (black) and 1 Hz (blue) wind data. (a) Time series comparison from a typical flux run at 460 m on 1 Sep 2004 in hurricane Frances. (b) Frequency spectra from the flux run of (a). (c) Frequency cospectra of the horizontal momentum flux. (d) Cumulative sum or ogive of the spectra. (e) Cumulative sum or ogive of cospectra of the horizontal momentum flux.

Figure 4: Horizontal momentum flux ($|F_h|$) as a function of the mean wind speed at the flight level for all flux runs in Hurricanes Allen (Δ), David (x), Hugo (o) and Frances (+). The sign of the momentum flux is shown in Table 1.

Figure 5: Comparison of the magnitudes of the horizontal ($|F_h|$) and vertical ($|\tau_v|$) momentum fluxes. Symbols are as in Fig. 4.

Figure 6: Horizontal eddy diffusivity (K_h) as a function of mean wind speed at flight level for all flux runs in Hurricanes Allen (Δ), David (x), Hugo (o) and Frances (+).

Figure 7: Horizontal mixing length (L_h) as a function of mean wind speed at flight level for all flux runs in Hurricanes Allen (Δ), David (x), Hugo (o) and Frances (+). The thick black curve represents the bin-averaged values with 95% confidence interval. The bin width is 15 m s^{-1} and the averaging begins at 7 m s^{-1} . The grey dashed line shows the mean value of all the data. The black * shows the average value of the data outside the eyewall region, while the black diamond shows the average value of the data for the eyewall legs.

Figure 8: Horizontal momentum flux cospectra (a) and the cumulative sum of the cospectra for a typical eyewall flux run.

Table Caption:

Table1: Summary of data and calculations for all flux runs presented here. The variables are storm name, date, start time (T_s in UTC hour and minute), end time (T_{nd}), mean altitude (z in m), mean flight-level wind speed (w_s in ms^{-1}), horizontal eddy momentum flux (F_h in N m^{-2}), mean strain rate (S_h in 10^{-3} s^{-1}), mean deformation (D_h in 10^{-3} s^{-1}), horizontal eddy diffusivity (K_h in $\text{m}^2 \text{ s}^{-1}$), and horizontal mixing length (L_h in m). Signs of momentum flux and strain rate are included.

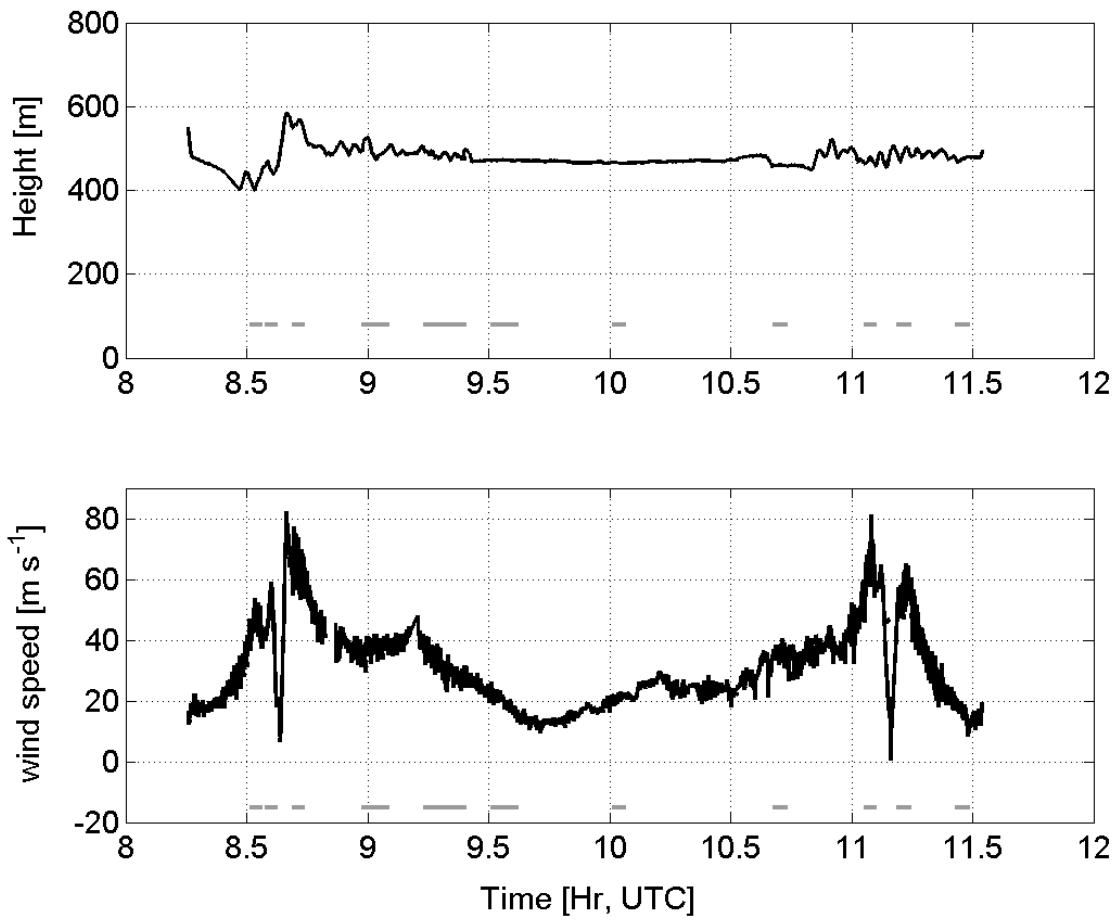


Figure 1: Aircraft altitude (a) and flight-level wind speed (b) during Hurricane David on 6 August 1980, 8-12 UTC. The gray lines denote the flux runs investigated herein.

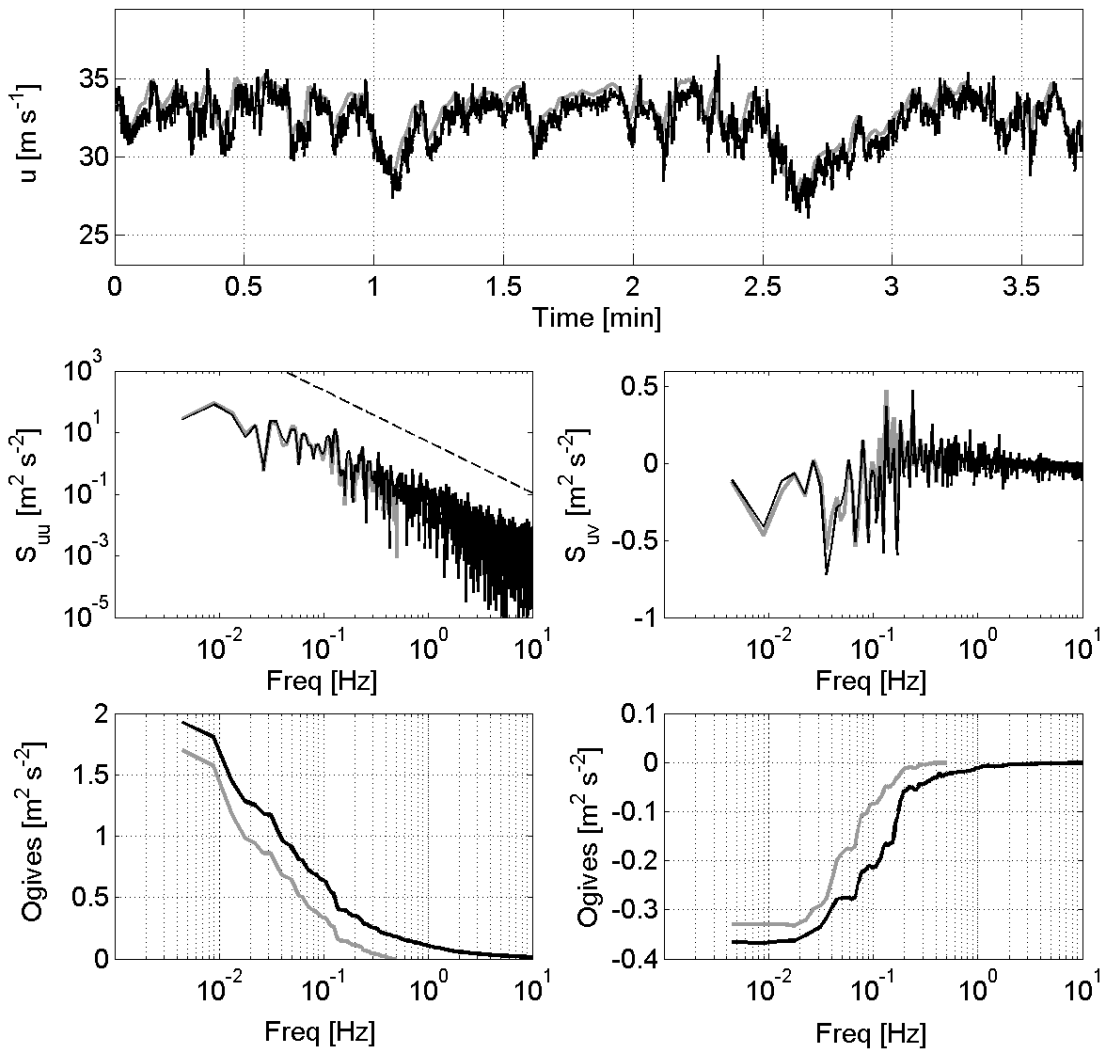


Figure 3: Comparison of the 40 Hz (black) and 1 Hz (blue) wind data. (a) Time series comparison from a typical flux run at 460 m on 1 Sep 2004 in hurricane Frances. (b) Frequency spectra from the flux run of (a). (c) Frequency cospectra of the horizontal momentum flux. (d) Cumulative sum or ogive of the spectra. (e) Cumulative sum or ogive of cospectra of the horizontal momentum flux.

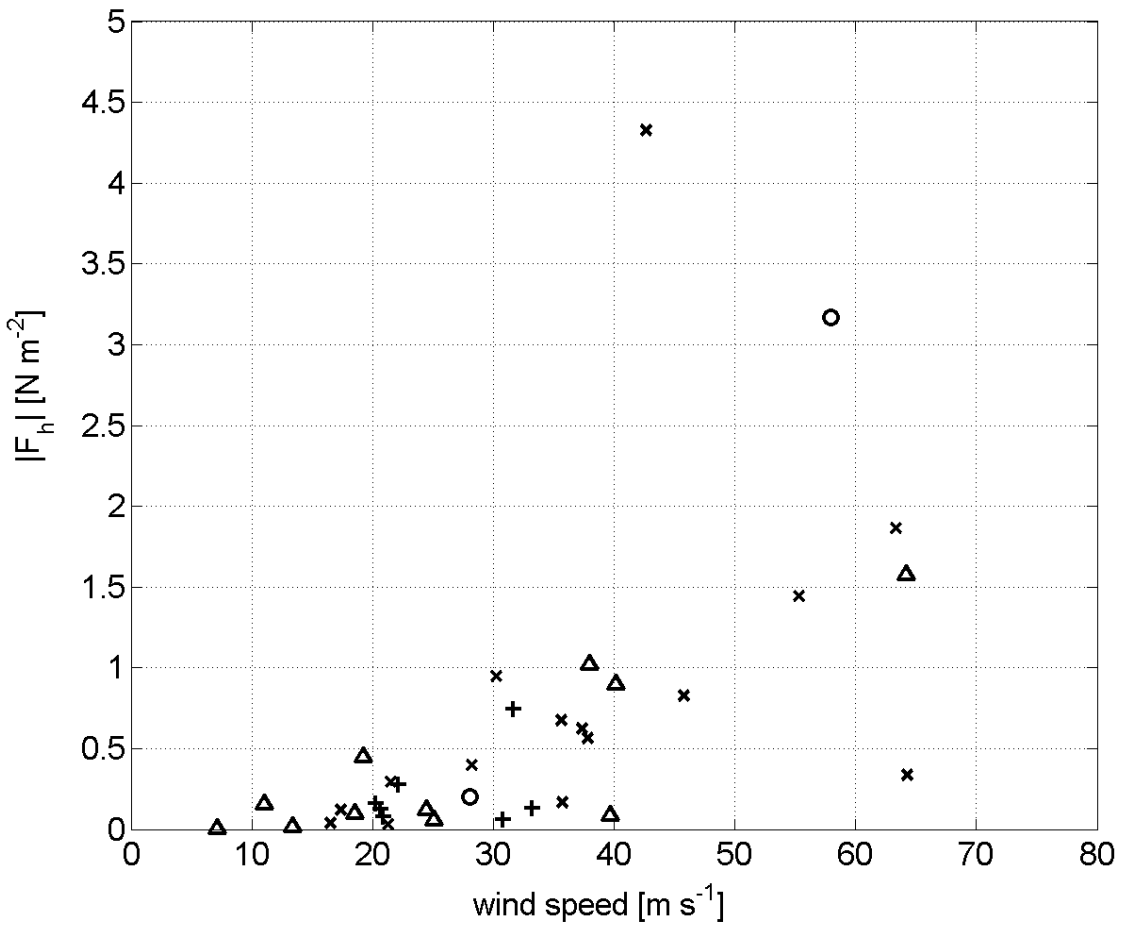


Figure 4: Horizontal momentum flux ($|F_h|$) as a function of the mean wind speed at the flight level for all flux runs in Hurricanes Allen (Δ), David (\times), Hugo (\circ) and Frances ($+$). The sign of the momentum flux is shown in Table 1.

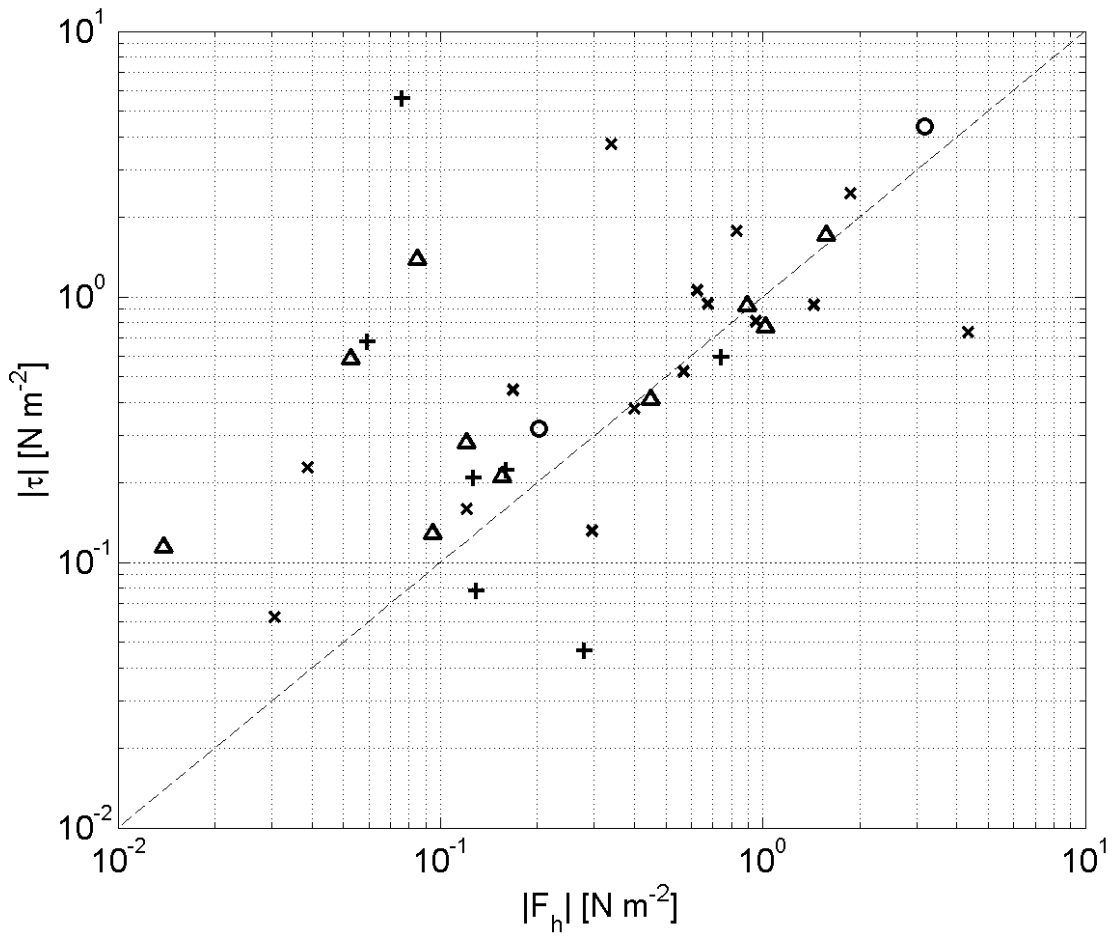


Figure 5: Comparison of the magnitudes of the horizontal ($|F_h|$) and vertical ($|\tau|$) momentum fluxes. Symbols are as in Fig. 4.

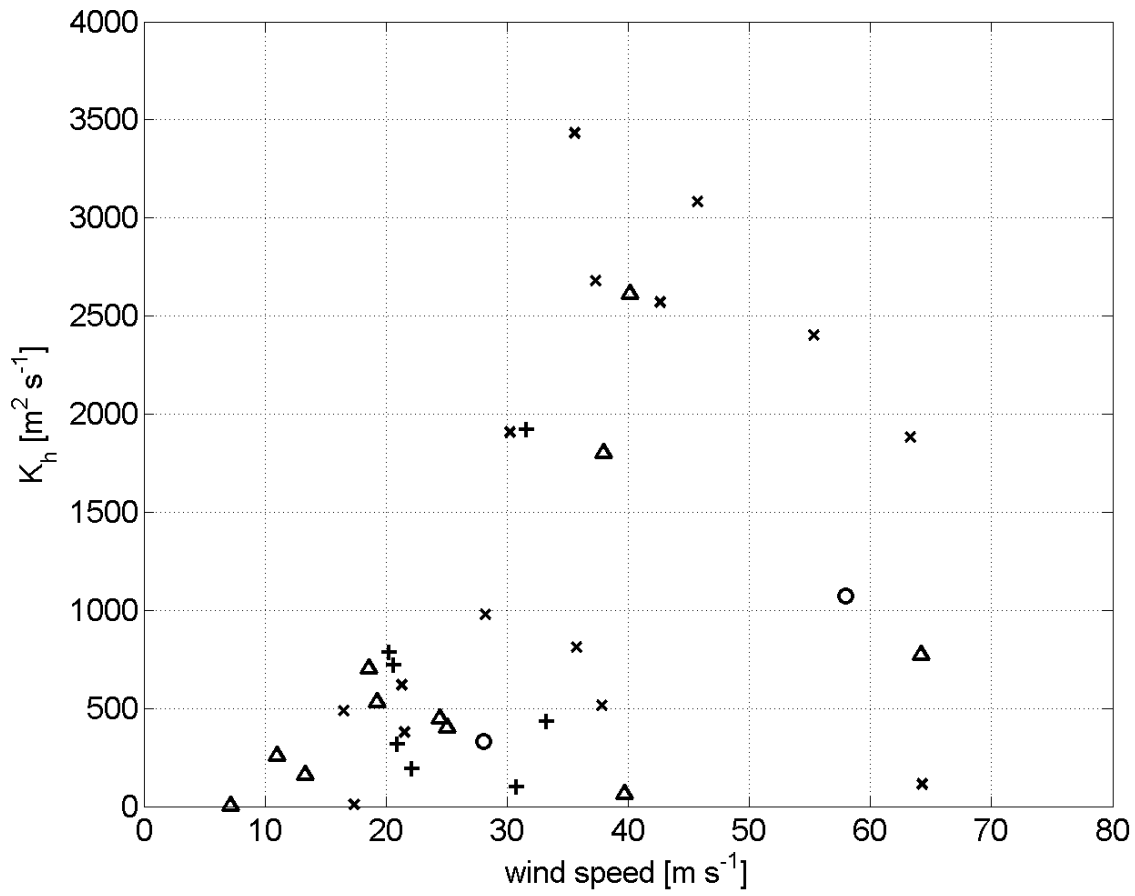


Figure 6: Horizontal eddy diffusivity (K_h) as a function of mean wind speed at flight level for all flux runs in Hurricanes Allen (Δ), David (x), Hugo (o) and Frances (+).

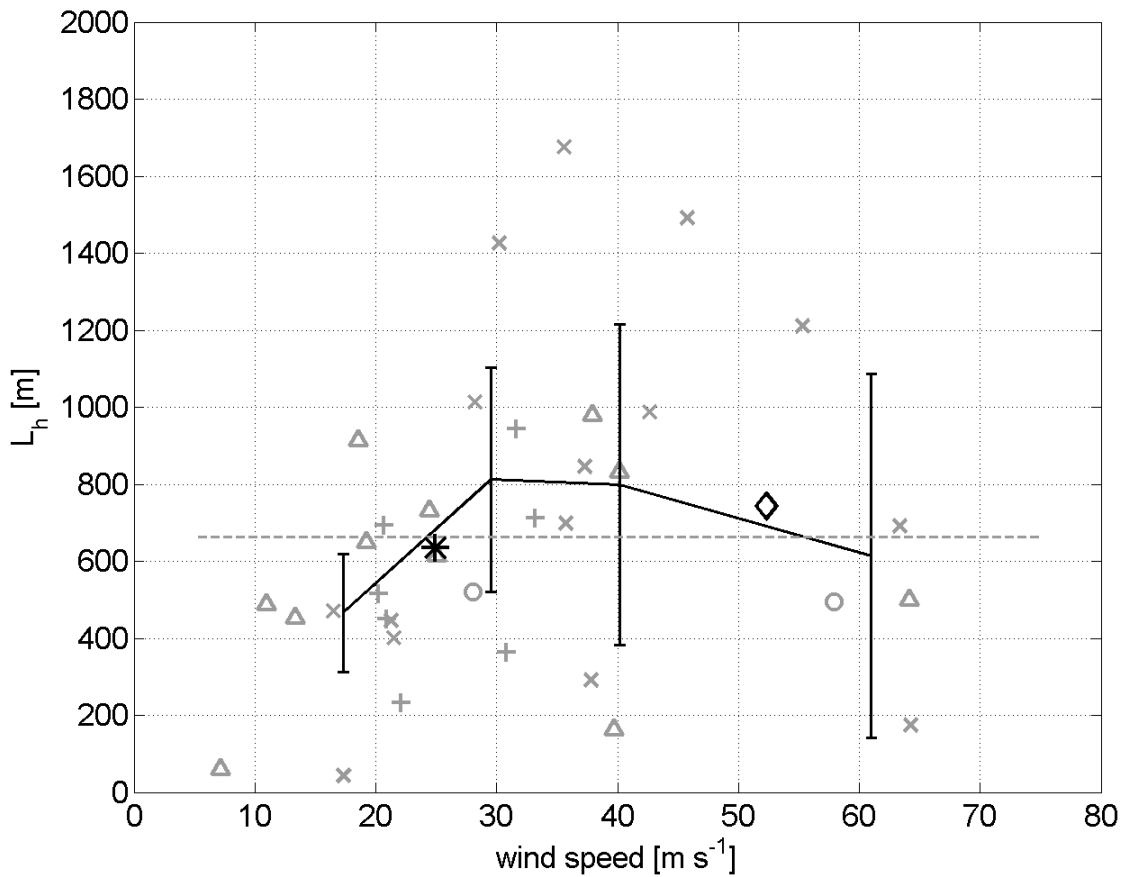


Figure 7: Horizontal mixing length (L_h) as a function of mean wind speed at flight level for all flux runs in Hurricanes Allen (Δ), David (x), Hugo (o) and Frances (+). The thick black curve represents the bin-averaged values with 95% confidence interval. The bin width is $15 m s^{-1}$ and the averaging begins at $7 m s^{-1}$. The grey dashed line shows the mean value of all the data. The black * shows the average value of the data outside the eyewall region, while the black diamond shows the average value of the data for the eyewall legs.

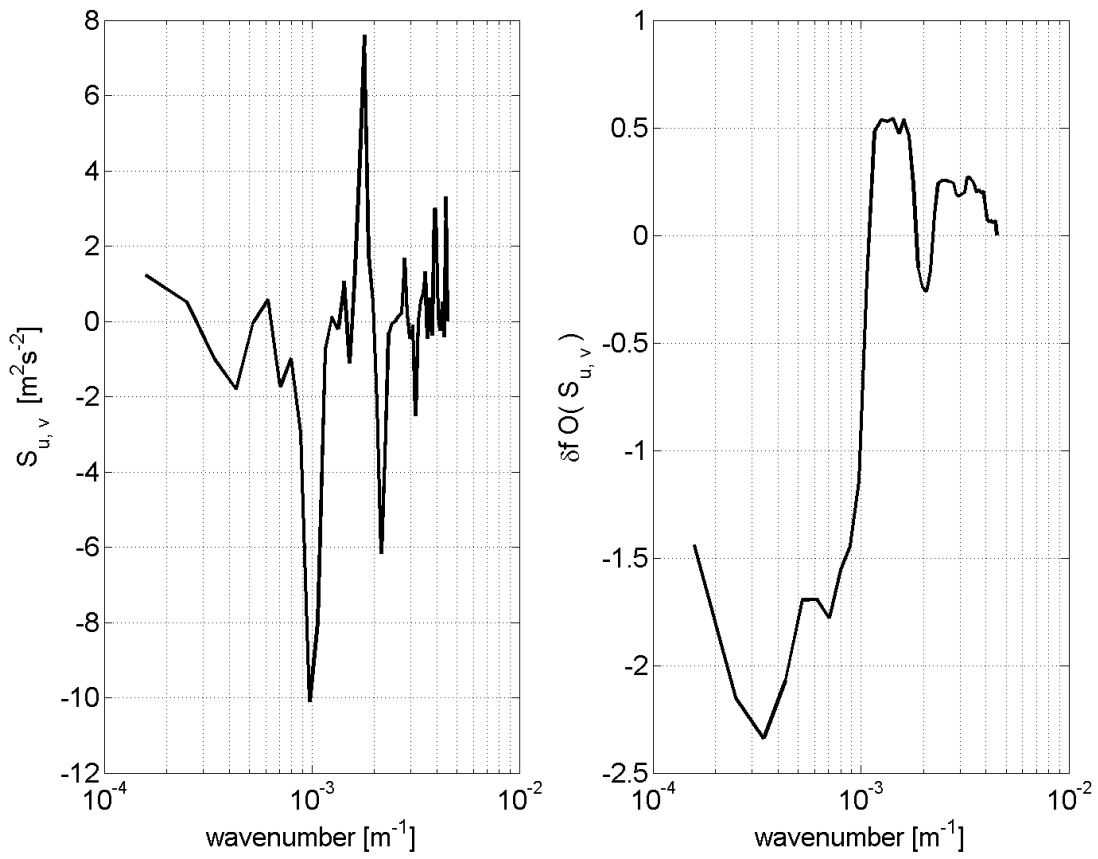


Figure 8: Horizontal momentum flux cospectra (a) and the cumulative sum of the cospectra for a typical eyewall flux run.

Table1: Summary of data and calculations for all flux runs presented here. The variables are storm name, date, start time (T_s in UTC hour and minute), end time (T_{nd}), mean altitude (z in m), mean flight-level wind speed (ws in ms^{-1}), horizontal eddy momentum flux (F_h in $N\ m^{-2}$), mean strain rate (S_h in $10^{-3}\ s^{-1}$), mean deformation (D_h in $10^{-3}\ s^{-1}$), horizontal eddy diffusivity (K_h in $m^2\ s^{-1}$), and horizontal mixing length (L_h in m). Signs of momentum flux and strain rate are included.

Storm Name	Date	T_s	T_{end}	z	ws	F_h	S_h	D_h	K_h	L_h
David	19790830	85837	90156	504.79	37.32	0.63	0.21	3.74	2680.30	846.11
David	19790830	90157	90516	488.01	37.81	0.57	0.98	6.07	515.85	291.60
David	19790830	91356	91715	486.77	35.59	-0.68	-0.17	1.22	3434.11	1676.11
David	19790830	91716	92035	481.54	30.23	-0.95	-0.44	0.94	1908.33	1426.23
David	19790830	92036	92355	481.72	28.20	-0.40	-0.36	0.95	980.13	1013.64
David	19790830	93036	93355	471.58	21.51	-0.30	-0.69	2.35	378.46	401.30
David	19790830	93356	93715	471.03	17.35	-0.12	-10.12	5.42	10.60	44.24
David	19790830	100036	100355	465.23	21.27	-0.03	0.04	3.11	619.77	446.32
David	19790830	104036	104355	459.25	35.72	-0.17	0.18	1.67	813.04	698.64
David	19790830	112546	112905	472.86	16.49	-0.04	0.07	2.20	488.90	470.90
David	19790830	83047	83346	417.99	45.74	0.83	0.24	1.39	3083.53	1492.08
David	19790830	83437	83726	451.76	42.65	-4.33	1.50	2.63	2571.51	987.99
David	19790830	84117	84416	558.78	64.27	0.34	2.59	3.78	115.83	174.94
David	19790830	110306	110605	464.93	63.32	1.86	0.88	3.94	1882.36	691.49
David	19790830	111116	111435	486.56	55.30	1.44	-0.53	1.64	2403.38	1211.56
Allen	19800806	150450	150809	482.61	24.48	-0.12	-0.24	0.83	445.02	730.35
Allen	19800806	150820	151139	442.64	25.08	-0.05	0.12	1.06	400.51	615.16
Allen	19800806	153530	153849	473.05	18.57	-0.09	0.12	0.84	703.39	914.32
Allen	19800806	154210	154529	497.82	13.35	0.01	0.08	0.78	159.51	451.70
Allen	19800806	154610	154909	498.52	11.02	-0.16	-0.54	1.08	256.50	486.57
Allen	19800806	154950	155329	498.27	7.17	-0.00	-0.53	1.29	4.53	59.13
Allen	19800806	161250	161609	422.07	19.27	-0.45	0.75	1.26	531.64	648.58
Allen	19800806	164820	165139	847.66	40.15	0.89	-0.30	3.77	2609.63	832.02
Allen	19800806	151600	151939	484.59	39.72	0.09	-1.18	2.41	63.88	162.73
Allen	19800806	152820	153319	576.14	37.94	-1.02	-0.50	1.88	1801.93	978.07
Allen	19800806	163220	163719	844.92	64.19	1.57	1.82	3.08	769.74	500.22
Hugo	19890815	172002	172401	458.78	28.07	-0.20	-0.54	1.23	331.39	519.61
Hugo	19890815	172450	172741	437.43	57.94	-3.17	-2.63	4.37	1072.55	495.52
Frances	20040901	174040	174444	481.27	20.90	-0.08	-0.21	1.56	318.11	451.36
Frances	20040901	174444	174848	448.72	20.24	-0.16	-0.18	2.95	786.70	516.51
Frances	20040901	175353	175757	453.69	22.09	-0.28	1.29	3.52	192.25	233.61
Frances	20040901	175959	180202	458.11	20.66	-0.13	-0.16	1.50	720.91	694.08
Frances	20040901	190505	190808	553.08	30.79	0.06	-0.52	0.77	101.68	362.76
Frances	20040901	191212	191515	452.41	33.21	0.13	-0.26	0.86	435.68	711.75